Pharmaceutical Sciences, 2023, 29(1), 111-122
doi:10.34172/PS.2022.29
https://ps.tbzmed.ac.ir/

Research Article

Characterization and Biological Activities of Silver Nanoparticles Synthesized Using *Grewia tiliifolia* Vahl Leaf Extract

Sneha Desai K.[1], **Tarikere C. Taranath**[1*]

[1]*Environmental Biology and Green Nanotechnology Laboratory, P. G. Department of Studies in Botany, Karnatak University, Dharwad 580003, Karnataka, India.*

Article Info

Article History:
Received: 22 Feb 2022
Accepted: 02 Jul 2022
ePublished: 14 Jul 2022

Keywords:
-Anticancer
-Antioxidant
-Antituberculosis
-Green synthesis
-Lung cancer
-*Mycobacterium tuberculosis*

Abstract

Background: An eco-friendly approach for the synthesis of noble metal nanoparticles employing various plant extracts has become of great interest in the field of nanotechnology. In the present study, the efficacy of *Grewia tiliifolia* leaf extract in reducing 1 mM silver nitrate to silver nanoparticles (AgNPs) has been reported for the first time. We also investigated the anticancer, antituberculosis and antioxidant activity.

Methods: Characterization of biosynthesized AgNPs using *G. tiliifolia* leaf extract was evaluated by different techniques. Efficacy of biosynthesized AgNPs using *G. tiliifolia* leaf extract was tested for cytotoxicity against A549 Lung cancer cell lines by MTT Assay and against the infectious agent *Mycobacterium tuberculosis* using MABA assay. Further antioxidant activity was evaluated by DPPH radical scavenging assay.

Results: The biosynthesis of AgNPs was evident by a color change of the reaction mixture from dark yellow to reddish-brown. Biofabricated AgNPs were further confirmed by characteristic surface plasmon absorption peak at 409 nm by UV-vis analysis. FTIR data reveals the presence of phytochemicals involved in bioreduction and biocapping of AgNPs, XRD analysis depicted the crystallographic nature of AgNPs. Further, size, charge, and polydispersity nature were studied using DLS (40.2 nm with polydispersity index 0.361) and Zeta potential (-35.8 mV). The morphology of AgNPs was determined by TEM analysis with a size ranging from 11-34 nm. The plant-derived AgNPs exhibited a cytotoxic effect on the lung cancer cell line with an IC_{50} value of 23.45 µg/ml and were also found to be effective against *M. tuberculosis* with a MIC of 6.25 µg/ml in comparison to the leaf extract (MIC 50 µg/ml). Antioxidant activity observed by AgNPs was moderate with IC_{50} value of 49.60 µg/ml.

Conclusion: The findings indicate that the AgNPs synthesized from leaf extract of *G. tiliifolia* are eco-friendly, cost-effective, non-toxic and can be effective natural anticancer, antituberculosis and antioxidant agents.

Introduction

Tuberculosis (TB) is a contagious disease that is one of the top ten causes of mortality worldwide (Ranking above HIV/AIDS) and the prime reason for death caused by a single infectious pathogen.[1] Despite years of studies, more than 4300 fatalities every day worldwide continue to be accountable for tuberculosis produced by *Mycobacterium tuberculosis*.[2] Reasons that cause the formation of Multi-Drug Resistant (MDR) tuberculosis and of more severe forms called Extensively Drug-Resistant (XDR) include prolonged therapy, a high pill load, low compliance, and strict administration schedules.[3] The awareness about the growth of MDR and XDR strains and the absence of successful treatment alternatives enhance the need for novel and effective anti-TB medicines to solve the drug resistance problem, ease up therapy and exert control. Another major cause of morbidity and mortality is cancer. Cancer instances have increased significantly in recent years, and most of the time, it results in death. According to the WHO (World Health Organization), there were 2,206,771 new lung cancer cases among all forms of cancer documented in 2020, with total mortality of 1,796,144.[4] Many treatments have been used to fight cancer, including chemotherapy, immunotherapy, and radiotherapy however, these techniques are incapable of limiting adverse effects.[5] The most challenging problem in cancer treatment is preventing normal cells from being destroyed while treating malignant cells.[6] In this regard, nanotechnology may emerge as one of the most promising options for developing more effective medication delivery methods for TB and cancer therapy.

Recently, exploration in the sector of nanotechnology

*Corresponding Author: Tarikere C. Taranath, E-mail: tctaranath@gmail.com

has been growing to a greater extent due to its appreciable contribution over multiple fields, involving biotechnology, microbiology, material sciences, engineering, environmental sciences, computer sciences, therapeutic work, and so forth.[7] Silver nanoparticles (AgNPs) are essential members of noble metal nanoparticles (NPs), especially since the antimicrobial properties of silver were already well known in the medical sector.[8] Scientists have been continuously exploring new nanoparticle synthesizing methods for several years, including chemical synthesis,[9] physical synthesis,[10] photochemical processes,[11] and biosynthesis.[12] Conversely, chemical, physical, and photochemical methods produce hazardous toxic substances. Therefore, the green approach for the synthesis of AgNPs has been explored for over a decade as an environment-friendly synthesis method. Plants contain an array of phytochemicals that serve as a converter, coating agent, and stabilizer for transforming metal NPs from metallic ions resulting in the generation of preferable nanoparticles with highly specific properties.[13] Metabolites from different plant parts such as leaves,[14] stems,[15] roots,[16] fruits,[17] flowers,[18] bark,[19] and seeds[20] have shown an influential role as reducing agents in the process of NPs biosynthesis. The green synthesis of AgNPs using several plant extracts like *Leucas aspera*,[21] *Aloe vera*,[22] *Azadirachta indica*,[23] *Catharanthus roseus*,[24] *Aegle marmelos*,[25] *Jasminum officinal*,[26] *Phyllanthus emblica*,[27] *Acalypha indica*,[28] etc. have been reported in the previous studies.

The present investigation focuses on the environmentally sustainable AgNPs synthesis utilizing aqueous leaf extract of *Grewia tiliifolia* Vahl (Gt). The abundance of Gt is discovered in western and eastern ghats belonging to the family Malvaceae. The compounds present in the Gt leaf are alkaloids, saponins, tannins, triterpenoids, carbohydrates, phenols, steroids, flavonoids, and quinones.[29] Among these main active compounds are triterpenes : Friedelin, Lupel and Betulin. Compounds like Gulonic acid γ-Lactone and D-erythro-2-hexenoic acid γ-Lactone are found in the preliminary phytochemical study.[30]

Thamizh *et al.*[31] reported the antioxidant potential on different radical systems such as superoxide radicals, hydroxyl radicals and nitric oxide radicals and also reported the tumor cell suppression potential of methanolic extract of Gt bark on 3 different cancer cell lines i.e., MCF-7 (breast cancer), HepG2 (hepatocancer) and A549 (lung cancer) in the model system. Dicson *et al.*[32] stressed on the toxicological profile of the methanolic extract of Gt leaves through *in vitro* (cytotoxic, mutagenic, genotoxic) and *in vivo* (acute and sub-acute). Khadeer *et al.*[33] evaluated *in vitro* antioxidant and *in vivo* prophylactic effect of two γ-lactones isolated from Gt against hepatotoxicity in carbon tetrachloride intoxicated rats. Vivek *et al.*[34] reported antioxidant activity by nitric oxide radical inhibition and DPPH radical scavenging activity, antimicrobial activity on *B. sterarothermophilus, B. arrogeuosa, B. coagulans, K. Pneumoniae, L. licjmani, shijell* and *P. cepacian* and cytotoxic activity on Vero and Hep-2 cell lines. Various tribal groups in India use aqueous leaf extract of this plant as an indigenous remedy to treat dermatitis and as a diuretic.[32]

Despite these medicinal properties, there are no reports on the use of Gt in the synthesis of AgNPs. Hence, an attempt has been made for AgNPs synthesis by using *G. tiliifolia* leaf extract (GtLE). Further, Biological activities such as antioxidant activity, anticancer activity on lung cancer (A549) cell line and antituberculosis activity against *Mycobacterium tuberculosis* (H37 RV strain) were investigated.

Materials and Methods

Sample collection and preparation of extract

Green and healthy leaves of Gt were collected from the surroundings of Khanapur (Dist.-Belgaum, Karnataka, India). To remove dirt, the leaves collected were cleaned with tap water thrice and then rinsed with deionized water. The plant extract was prepared by adding 10 g of washed and chopped leaves in 100 mL of distilled water in 250 mL of Erlenmeyer flask and then boiled for 45 minutes. The extract was allowed to cool down to ambient conditions, and then finally filtered using Whatman filter paper No.1. The obtained clear GtLE was maintained at 4°C for the subsequent production of AgNPs.

Biofabrication of AgNPs

For the fabrication of AgNPs, the method followed which is described earlier by Sarkar and Kotteeswaran[35] with some modifications. 1 mM silver nitrate ($AgNO_3$) solution was prepared in distilled water. 5 mL of leaf extract was added to 95 mL of $AgNO_3$ solution. After 15 minutes, the formed AgNPs were validated by visual observation of color change from dark yellow to reddish-brown. The pH of the resulting solution was raised to 8.5 by adding 1 N NaOH dropwise. The solution was incubated in a water bath for 15-20 minutes at a temperature of 60-80°C and stored at room temperature for the reaction to complete synthesis. The reaction mixture was centrifuged three times at 14,500 rpm (Eppendorf centrifuge-5424) for 30 minutes, followed by redispersion of the residue in de-ionized water to purify the AgNPs synthesized. Pellets collected after centrifugation were kept in an oven to dry at 60°C in a watch glass. The purified nanoparticles were then characterized and used for anticancer and antituberculosis activity.

Characterization of AgNPs

The initial characterization of AgNPs synthesized using aqueous leaf extract of *G. tiliifolia* (GtL-AgNPs) was tracked by evaluating the UV-Visible (UV-Vis) spectrum (JASCO V-670 UV-Vis -NIR Spectrophotometer) at 200-600 nm, diluting a fraction of the NPs sample in distilled water, here the distilled water was used as blank. Analytical techniques like DLS (Dynamic Light Scattering) with PDI (Polydispersity Index) and zeta potential (HORIBA SZ-100) were used to find out the average diameter of NPs

dispersed in aqueous solution and stability of AgNPs respectively. To identify the phytochemicals involved in the capping of AgNPs NICOLET NXR FT Raman Spectrometer (4000 cm^{-1} to 500 cm^{-1}) was used. To analyze the crystalline planes of AgNPs, X-Ray Diffraction (XRD) was carried out using RIGAKU SmartLab SE X-ray diffractometer. HR-TEM (High-Resolution Transmission Electron Microscopy) with SAED (Selected Area Electron Diffraction) analysis was used to know the morphology, crystallographic structure of AgNPs, and d-spacing of crystal planes using the instrument JEOL/JEM 2100.

Biological activities

Antioxidant activity: DPPH radical scavenging assay

Free radical scavenging activity of GtL-AgNPs was evaluated by using its potentiality to trap the 2,2-diphenyl-1-picrylhydrazyl (DPPH) free radicals following the method described by Choi *et al.*[36] varying concentration of AgNPs (10-50 µg/ml) was prepared in de-ionized water. 1 ml of 0.1 mM DPPH prepared in methanol is added to this. The tubes are incubated in dark for 30mins at room temperature. After incubation, the absorbance is recorded at 517 nm. Control consists of DPPH in methanol without the addition of a test sample. Ascorbic acid has been used as a standard. Further Radical scavenging activity was measured and calculated as follows:

Scavenging effect (%) =[(Ac-As)/Ac] ×100

Where Ac is the Absorbance of Control, As is the Absorbance of Standard/Sample

In-vitro Anticancer activity (Lung cancer- A549)

Using the standard colorimetric MTT (3-(4,5-dimethylthiazol-2-yl)-2,5-dimethyl tetrazolium bromide dye) test (Sigma, St. Louis, MO, USA). The impact of GtLE and GtL-AgNPs on the proliferation of non-small cell lung cancer (A549) cells was evaluated (Sigma, St. Louis, MO, USA). A549, lung cancer cell lines were procured from National Centre for Cell Sciences (NCCS), Pune, India. The MTT method followed which was described previously by Shettar *et al.*[37] with some modifications. In brief, the monolayer cell culture was Trypsinized and seeded into 96-well microtiter plates (Falcon, Becton– Dickinson, Franklin Lakes, NJ, USA) in DMEM (Dulbecco's Modified Eagle Medium) containing 10% FBS (Fetal Bovine Serum). The cells were cultured for 24 hours at 37°C in a 5% CO_2 incubator. The media within the wells was replaced after 24 hours of seeding with fresh medium and cells treated with different concentrations of GtLE and GtL-AgNPs (10–50 µg/mL) and incubated for another 24 hours. MTT solution was added to each well, and the plates were incubated for 3 to 4 hours to determine cell viability. The MTT solution was then discarded, 100 µL of DMSO (dimethyl sulfoxide) was added, and the quantity of formazan produced was measured on a Model 680 Microplate Reader (Bio-Rad Laboratories, Inc., Hercules, CA, USA) at 570 nm. The % cell viability was calculated by applying the following formula:

Cell viability (%) = OD of test sample / OD of control × 100, and the concentration of test sample required to inhibit cell growth by 50% (IC_{50}) values were derived using cell line dose-response curves. This test is based on the reduction of MTT to a purple formazan resulting from mitochondrial dehydrogenase in intact cells.

In-vitro antituberculosis activity (Mycobacterium tuberculosis)

Using the MABA (Microplate Alamar Blue Assay), the *in-vitro* efficacy of GtLE and GtL-AgNPs was assessed against the H37 Rv strain of *Mycobacterium tuberculosis* (ATCC No- 27294). The MABA method was followed as described previously by Lourenço *et al.*[38] In brief, to reduce medium evaporation within test wells throughout incubation, 200 µL of sterile distilled water was introduced into every edging well of a sterile 96 well plate. The 96 well plate were supplied with 100 µL of Middlebrook 7H9 broth. The GtLE and GtL-AgNPs were serially diluted on the plate directly. The final GtLE and GtL-AgNPs concentrations examined from 0.2 to 100 µg/mL. The plates were wrapped and sealed with parafilm before being incubated at 37°C for five days. The plate was filled with 25 µL of freshly prepared Alamar Blue reagent (1:1) and 10% Tween 80 after five days and incubated again for 24 hours. A blue-colored

Figure 1. Visual observation of color change during the AgNPs synthesis. **(a)** $AgNO_3$, **(b)** *G. tiliifolia* leaf extract, **(c)** reaction mixture of AgNO3 and extract, **(d)** AgNPs solution at pH 4.2, **(e)** AgNPs solution at pH 8.5.

well showed no bacterial growth, but a pink-colored well indicated growth. The MIC (Minimum Inhibitory Concentration) was defined as the lowest medication concentration that inhibited the change of color from blue to pink. As a comparison, the drugs Isoniazid, Ethambutol, Pyrazinamide, Rifampicin, and Streptomycin were used.

Statistical analysis

All the experiments were conducted in triplicates and the results were expressed as the Mean ± Standard error. Multiple comparison test was used to show significant difference using Two-way ANOVA followed by the Tukey test. All the data were analyzed using GraphPad Prism (version 9.0.0) and Microsoft Office Excel 2019. A value of $p<0.05$ was considered to assign a statistically significant difference.

Results and discussion

Characterization studies of GtL-AgNPs

Visual analysis and UV-Vis spectroscopy

Green synthesized AgNPs solution changed the color from light yellow to reddish-brown after 15 minutes due to the reduction of $AgNO_3$ to AgNPs by active compounds found in GtLE (Figure 1), which is the key and noteworthy evidence for AgNPs formation. In the presence of oxygen, such as in $AgNO_3$, primary and secondary metabolites lose their electron and become oxidized via standard cellular procedures. $AgNO_3$ solution, which has positive ions (Ag^+) converts to a zero valent state (Ag^0), when plant extract is added to it. Phenolic compounds like flavonoids and tannins present in the plant act as reducing agents ($Ag^+ \rightarrow Ag^0$) and play an essential role in the stability of AgNPs[6]. Al-Shmgani *et al.*[39] used *Catharanthus roseus* extract for AgNPs synthesis using an alkaloid of indole type, which acted as a reducing and stabilizing agent. Similarly, Majeed *et al.*[40] reported the synthesis of AgNPs using *Artocarpus integer* leaf extract and synthesized spherical NPs of 5.76 nm to 19.1 nm.

The absorption spectra (UV-Vis) of GtL-AgNPs showed SPR (Surface Plasmon Resonance) peaks at 426 nm (pH 4.2) and 409 nm (pH 8.5) (Figure 2). Broad peaks at longer wavelengths usually imply a rise in particle size, while a narrow peak at shorter wavelengths indicates the development of smaller AgNPs.[41] In our current research at 409 nm, a sharp and relatively narrow absorption was observed, indicating the development of high-quality AgNPs. According to the literature, an acidic pH promotes the formation of larger particles, while an alkaline pH promotes the formation of smaller particles.[42] The same results have been observed in the present study, where pH 4.2 produces larger particles while pH 8.5 produces smaller particles with good stability and bulk synthesis. As a result, pH 8.5 was selected for further study.

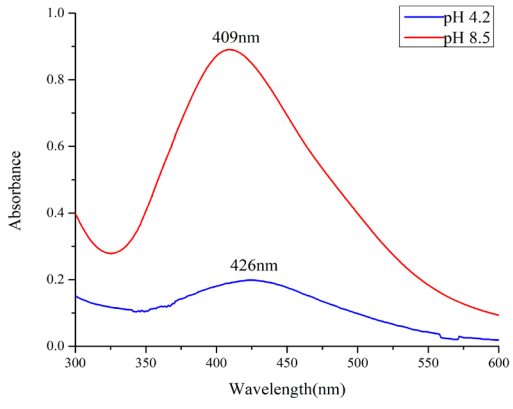

Figure 2. UV-Visible Spectra of synthesized AgNPs using *G. tiliifolia* leaf extract at pH 4.2 and pH 8.5.

DLS and zeta analysis (surface charge)

The hydrodynamic size and polydispersity index (PDI) of GtL-AgNPs were investigated using the DLS technique. Zeta potential was used to know the surface charge and stability of GtL-AgNPs. As seen in Figure 3a, the mean hydrodynamic size of GtL-AgNPs was 63.4 nm, with Z average of 40.2 nm, and the PDI value was found to be 0.361. If the PDI value is less than 0.1, then the particles are monodispersed, whereas values more than 0.1 may indicate polydisperse particle size distributions.[43] In Figure 3b zeta potential was observed to be -35.8 mV. Stable particles are those in suspension with a zeta potential greater than +30 mV or less than -30 mV.[44] The findings indicate that GtL-AgNPs are stable in a colloid system. This characteristic indicates that plant extract is effective as a natural stabilizer.

FT-IR

The FT-IR data reveals phytoconstituents involved in the synthesis process of AgNPs. Figure 4a represents the spectrum obtained from GtLE and GtL-AgNPs. The peaks at 3409.55, 2924.31,1620.62, 1396.55, 1112.61, 896.58, and 719.71 cm^{-1} represent the phytocompounds present in the GtLE whereas the vibrations at 3410.24, 2921.95, 1615.31, 1384.07, and 1028.99 cm^{-1} represent the biomolecules involved in the stabilization process of AgNPs. The absorption band at 3409.55 and 3410.24 cm^{-1} denotes the hydroxy compounds of the O-H stretching region. The bending at 2924.31 and 2921.95 cm^{-1} indicates $-CH_2(CH_2)$ of lipids and proteins. The band 1620.62 and 1615.31 cm^{-1} belong to the ketone C=O stretching. 1396.55 cm^{-1} resulted from the O-H bending representing alcoholic groups. The C-O stretching, polymeric OH of cyclic ether assigned to the peak at 1112.61 cm^{-1} whereas phosphate ion assigned to the peak at 1028.99 cm^{-1}. The vibration at 896.58 and 719.71 cm^{-1} is because of aromatic phosphate and aliphatic chloro compounds, respectively. After the capping of the nanosilver, the bands shifted to other wavelengths signifying that the GtLE phytochemicals actively contributed to the stabilization process. The band's appearance was more noticeable and sharper at 1384 cm^{-1}, which could be attributed to the residual amount of $AgNO_3$.[45] The reasonable shift in the peak position specifies that the different phytochemicals existing in the

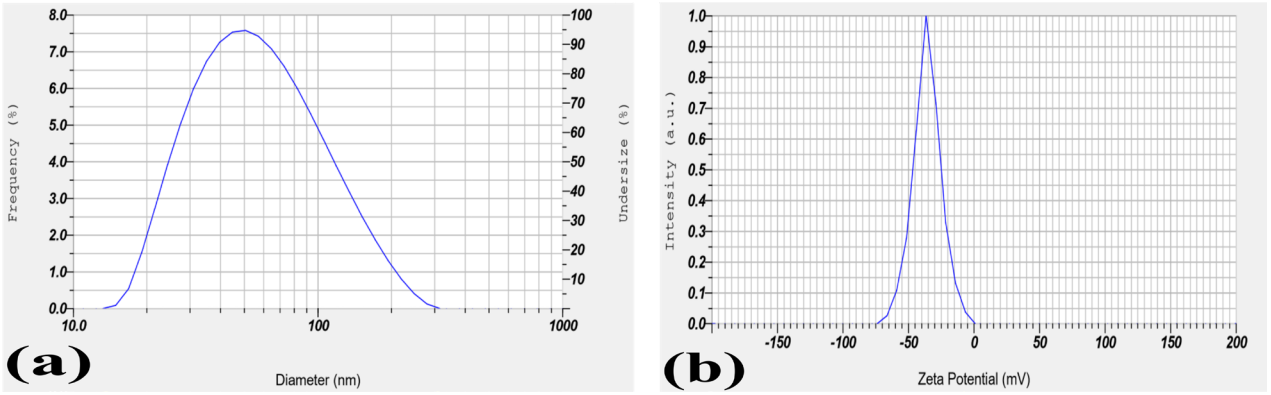

Figure 3. (a) DLS and (b) zeta potential graph of AgNPs synthesized from *G. tiliifolia* leaf extract.

GtLE are present in the GtL-AgNPs. As a result, plant extract components with OH and CO groups are crucial in the reduction and stability of NPs.[46] The result obtained was similar to the published data on FT-IR studies of GtLE prepared using distilled water, methanol, chloroform, Hexane, petroleum ether, acetone, ethyl acetate, and benzene by Devi and Battu.[47]

XRD

To understand the structural properties of GtL-AgNPs, XRD measurements were carried out. Figure 4b depicted the crystalline nature of GtL-AgNPs in the XRD pattern. Silver nanoparticles have a diffraction profile with extreme peaks at 2θ° of 38.19, 44.52, 64.54, 77.49, and 81.57, (220), (311), and (222) respectively. The standard data proved that the GtL-AgNPs produced were in the shape of face-centered cubic (fcc) crystalline lattice planes (ICDD Card No. 00-004-0783). Particle size was determined using the Scherrer equation on the x-ray peaks' width, and the calculated average size of crystallite was 12.03 nm from (111) plane. The results are consistent with previously published data of AgNPs synthesized using stem extract of *Cissus quadrangularis*.[48]

HR-TEM with SAED

Figure 5 shows the nature and size measurements of the formed AgNPs. The shape of the GtL-AgNPs was spherical and can be observed with the crystalline structure with visible lattice fringes and size ranges from 11 to 34 nm. FCC (Face-centered cubic) metallic silver may be distinguished by two different diffraction rings. In SAED pattern inner ring can be associated with (111) plane, a characteristic diffraction ring of AgNPs. The (220) reflection is most likely responsible for the outer ring. The results obtained in HR-TEM with SAED pattern agree with the XRD graph shown in Figure 4b.[49]

The variability in diameter values obtained from HR-TEM, XRD, and DLS analyses was primarily due to the sample preparation process. The particle size estimated by HR-TEM represents the actual diameter of the nanoparticles as measured in the sample's dry state., while the DLS procedure results in a greater hydrodynamic volume of nanoparticles in the hydrated state owing to solvent impact.[50]

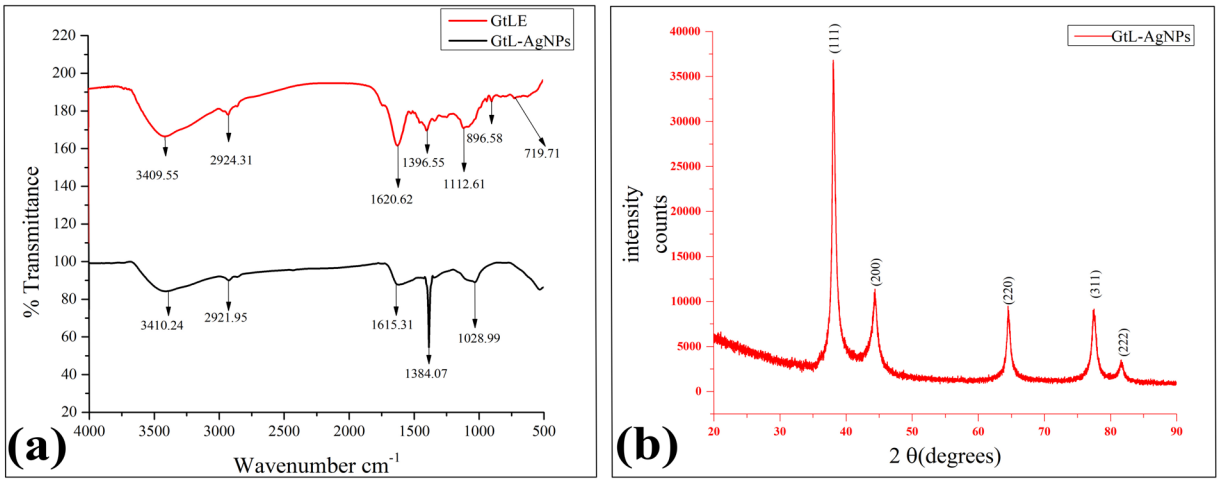

Figure 4. **(a)** FT-IR of *G. tiliifolia* leaf extract (GtLE) and AgNPs synthesized using *G. tiliifolia* (GtL-AgNPs). **(b)** X-Ray Diffraction pattern of AgNPs synthesized using leaf extract of *G. tiliifolia* with assigned silver peaks.

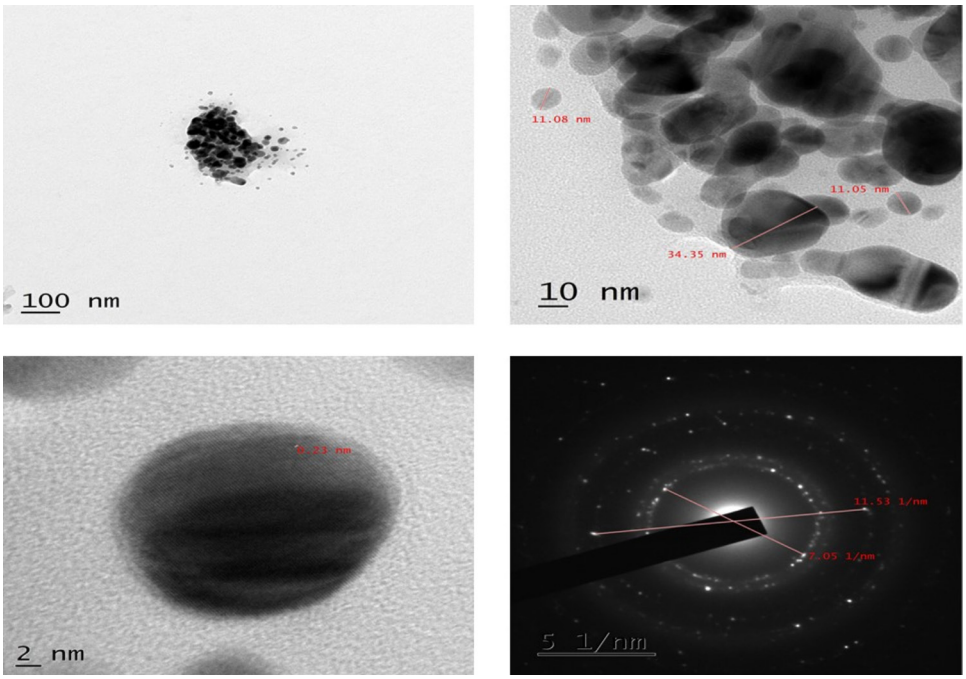

Figure 5. HR-TEM image of spherical green synthesized AgNPs from *G. tiliifolia* leaf extract at different grid locations showing lattice fringes along with SAED pattern.

Antioxidant activity: DPPH radical scavenging assay

The antioxidant activity of GtLE and GtL-AgNPs was evaluated by using DPPH free radical scavenging assay using Ascorbic acid as standard. The result of GtLE and GtL-AgNPs at different concentrations is shown in Figure 6a. Both AgNPs and Plant extract showed remarkable inhibitory activity against the DPPH radical. The % inhibition was increased with the increasing concentration in all the samples analyzed. Similar reports have been explained by Mata *et al.*[51] Comparison of numerical values presented in Table 1, and Figure 7a shows the significant difference ($p<0.05$) between the inhibition percentage of test samples GtLE, GtL-AgNPs and Ascorbic acid. Notably GtLE (IC_{50}=44.98 µg/mL) have shown stronger antioxidant activity in comparison to GtL-AgNPs (IC_{50}=49.60 µg/mL). It can be because the phytoconstituents present in the plant extract were more than the capped GtL-AgNPs. Plant extract can act as a reducing agent, so it readily donates electrons compared to AgNPs. which is well explained by Chahardoli *et al.*[52]

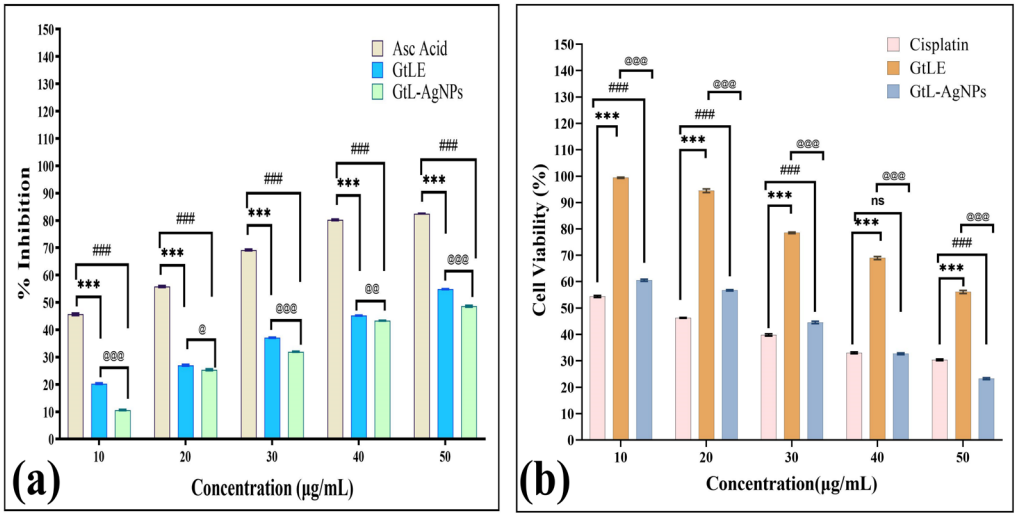

Figure 6. **(a)** Antioxidant activity of GtLE and GtL-AgNPs in comparison Ascorbic acid. *-Ascorbic acid vs. GtLE, #- Ascorbic acid vs. GtL-AgNPs, @-GtLE vs GtL-AgNPs. Values are mean ± SEM (n=3). Statistical significance using Two-way ANOVA. *p<0.05, **p<0.01, ***p<0.001, ns-non significant. **(b)** In vitro anticancer activity of GtLE and GtL-AgNPs in comparison cisplatin on A549 cell lines. Values are mean ± SEM (n=3). Statistical significance using Two-way ANOVA. *p<0.05, **p<0.01, ***p<0.001, ns: non significant. *-Cisplatin vs. GtLE, #- Cisplatin vs. GtL-AgNPs, @-GtLE vs GtL-AgNPs.

Table 1. Antioxidant activity of leaf extract of *G. tiliifolia* (GtLE) and silver nanoparticles synthesized using *G. tiliifolia* leaf extract (GtL-AgNPs).

No.	Concentrations (µg/mL)	% Inhibition (Mean ± SE)		
		Ascorbic acid	GtLE	GtL-AgNPs
1	10	45.67±0.39	20.29±0.22	10.66±0.17
2	20	55.85±0.32	27.03±0.29	25.36±0.29
3	30	69.20±0.23	37.13±0.14	31.98±0.15
4	40	80.25±0.24	45.20±0.08	43.34±0.08
5	50	82.54±0.07	54.89±0.11	48.60±0.30
	IC_{50}(µg/mL)	**12.98**	**44.98**	**49.60**

In-vitro anticancer activity

The effect of nanosilver on A549 cell growth was evaluated using the MTT test at various doses (10, 20, 30, 40, and 50 µg/mL). On A549 cells, both GtLE and GtL-AgNPs showed dose-dependent cytotoxicity. Increased concentration resulted in a reduction in cell viability (Figure 6b) and also showed a significant difference ($p<0.05$) between GtLE, GtL-AgNPs and the standard drug Cisplatin. The inhibitory concentration (IC_{50}) value of GtL-AgNPs was detected at a concentration of 23.45 µg/mL while GtLE at concentration of 56.31 µg/mL (Table 2). Microscopic pictures (Figure 7a-c) show that cells treated with Cisplatin, GtLE and GtL-AgNPs undergo morphological alterations. Venugopal *et al.*[53] reported a similar type of dose-dependent cytotoxicity of AgNPs produced using *Syzygium aromaticum* on A549 cell line with an IC50 value of 50 µg/mL. In relation to GtLE, synthesized GtL-AgNPs were found to be more effective in establishing a cytotoxic impact on lung cancer cell lines (A549). Silver nanoparticles may induce reactive oxygen species to form and disrupt cellular components, ultimately leading to cell death.[54] According to several *In-vitro* investigations, AgNPs can interfere with genes linked in cell cycle progression, as well as trigger DNA damage and death in cancer cells.[55] Alavi *et al.*[56] reported an anticancer mechanism of AgNPs which includes reprogramming pro-inflammatory cytokine cascade, redox pathways and immunosuppressive actions, further explained that AgNPs can reduce new blood vessels formation and also inhibit vascular endothelial growth factors.

In-vitro anti-tuberculosis activity

GtLE and GtL-AgNPs were assessed by MABA Assay against *M. tuberculosis* (H37Rv strain) as an Antituberculosis agent. This was studied in comparison with the MIC of reference medication drugs presented in Table 3. GtL-AgNPs were marked as very effective with a 6.25 µg/mL MIC, contrary to the MIC-50 µg/mL of GtLE. The effect of GtLE and GtL-AgNPs on the growth of *M. tuberculosis* may be seen in Figure 8. The color blue showed no growth of bacteria, while pink color indicated growth. It is worth noting that the GtL-AgNPs have more Anti-TB activity than GtLE. While the use of AgNPs in various antibacterial applications is widely established, the microbial action mechanism of *M. tuberculosis* is still unclear.

Abdel-Aziz *et al.*[57] threw light on the ultrastructural effect of nanoparticles on *M. tuberculosis* by tracking the physical interactions between chitosan/silver nanoparticles and *M. tuberculosis* cells using TEM. They further explained that there is a chitosan/silver nanoparticles deposition on the cell wall and after one day interaction led to cell membrane structural changes and damaging the bacterial cell wall and intracellular structures resulted in the death of mycobacteria. Similarly, Jung *et al.*[58] reported that AgNPs can easily enter the microbial body and damage all its intracellular structures, denaturing ribosomes and inhibit protein synthesis that can cause the death of bacteria. Singh *et al.*[59] reported phytogenic synthesis of AgNPs, AuNPs and Au-AgNPs using *Barleria prionitis*, *Plumbago zeylanica* and *Syzygium cumini* and extended their study on *M. tuberculosis* and *M. bovis*. They found that Au-AgNPs synthesized from *S. cumini* showed greater specificity towards mycobacteria. Patil BN and Taranath[60] studied the efficacy of zinc oxide nanoparticles synthesis using *Limonia acidisima* on *M. tuberculosis* as a potent

Table 2. Anticancer activity of leaf extract of *G. tiliifolia* (GtLE) and silver nanoparticles synthesized using *G. tiliifolia* leaf extract (GtL-AgNPs).

No.	Concentrations (µg/mL)	% Cell Viability (Mean±SE)		
		Cisplatin	GtLE	GtL-AgNPs
1	10	54.42±0.38	99.40±0.22	60.54±0.42
2	20	46.30±0.15	94.47±0.68	56.72±0.25
3	30	39.84±0.40	78.51±0.29	44.55±0.45
4	40	33.04±0.33	68.96±0.59	32.67±0.34
5	50	30.38±0.32	56.10±0.58	23.23±0.36
	IC_{50}(µg/mL)	**15.00**	**56.31**	**23.45**

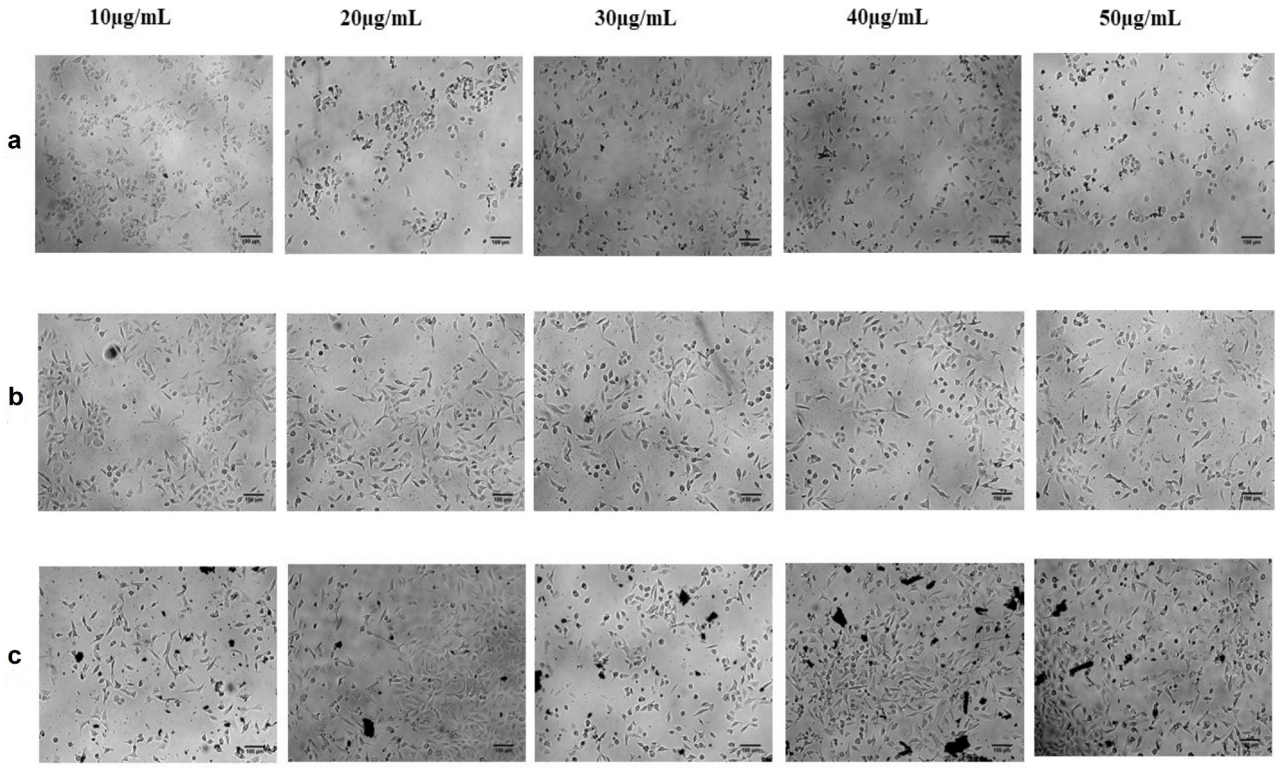

Figure 7. Microscopic images of In-vitro Anticancer activity on lung cancer (A549) cell lines. **(a)** A549 cell lines treated with standard drug Cisplatin, **(b)** A549 cell lines treated with *G. tiliifolia* aqueous leaf extract (GtLE), **(c)** A549 cell lines treated with nanosilver synthesized using aqueous extract of *G. tiliifolia* (GtL-AgNPs).

antimycobacterial tool. Further reported that growth of *M. tuberculosis* was inhibited by lipid peroxidation reaction, subsequently causing DNA damage, glutathione depletion, disruption of membrane morphology and electron transport chain, which leads to cell apoptosis. Alavi and Rai[61] explained the antibacterial functions of metal and metal oxide nanoparticles especially AgNPs. According to them adhesion to the cell membrane (alters membrane structure and permeability, leakage of cellular content and ATP, impair transport activity), mitochondrial dysfunction, destabilize ribosomes, denature proteins, interact with DNA, ROS generation and alters cell signaling these are some of the antibacterial functions which lead to the death of bacteria. However, AgNPs are known for inducing bactericidal effects as follows: 1) Bioactive ions release (for example Ag^+ ions), 2) Reactive oxygen species (ROS) generation, 3) multiple metabolic disruptions, 4) Direct interaction with the bacterial compounds (biofilm and the bacterial cell wall), 5) Cell wall and cytoplasm changes, 6) Genotoxicity, 7) Bacterial DNA replication inhibition, 8) Altered permeability and ionic bacterial membrane change.[62]

Conclusion

This is the first study to show an outstanding capability of leaf extract of *G. tiliifolia* as a reducing and capping agent for the synthesis of AgNPs since it could reduce the silver nitrate into very small and spherical-shaped AgNPs with a size range from 11 nm to 34 nm. It is a very easy, fast, reproducible, and environment-friendly approach that is an important contribution in the advancement of nanotechnology. Further characterization of GtL-AgNPs was done using UV-Vis spectroscopy, DLS, Zeta potential, FTIR, XRD and TEM with SAED. GtL-AgNPs showed remarkable antioxidant activity. Further, GtL-AgNPs have shown promising cytotoxic activity against A549 lung cancer cell line with IC_{50} value of 23.45 µg/mL which is compared with standard drug Cisplatin and GtLE. Antituberculosis activity of GtL-AgNPs against *M. tuberculosis* were investigated. GtL-AgNPs had the

Table 3. Comparative MICs of standard antitubercular drugs, *G. tiliifolia* leaf extract and AgNPs synthesized using *G. tiliifolia* leaves.

Parameters	Minimum Inhibitory concentration (MIC)						
	Standards					Test samples	
Samples	INH	ETM	PYZ	RIF	STR	GtL-AgNPs	GtLE
MIC(µg/mL)	1.6	3.2	3.125	0.8	0.8	6.25	50

INH: Isoniazid, ETM: Ethambutol, PYZ: Pyrazinamide, RIF: Rifampicin, STR: Streptomycin

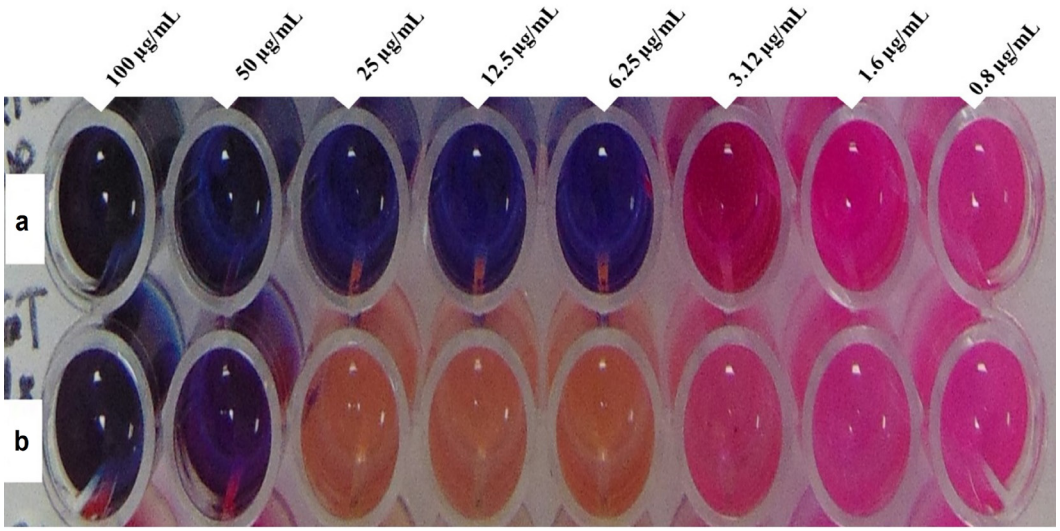

Figure 8. Microplate Alamar Blue Assay of AgNPs synthesized using *G. tiliifolia* leaves on *Mycobacterium tuberculosis*. **a)** *G. tiliifolia* mediated silver nanoparticles **b)** *G. tiliifolia* aqueous leaf extract.

ability to inhibit the growth of bacteria at 6.25 µg/mL. From the present findings, it can be concluded that silver nanoparticles synthesized using *G. tiliifolia* leaf extract can be used as an alternative to medications in pharmaceutical applications.

Acknowledgments

The authors thank the Chairman, P. G. Department of Studies in Botany, Karnatak University, Dharwad, Karnataka, India, for the laboratory facility. One of the authors is thankful to the University Research Studentship (KUD/SCH/URS/2019/352), Karnatak University Dharwad, for financial support. We also thank SAIF-USIC and DST-PURSE Programme Phase-II for providing the necessary instrumentation facility for the characterization of silver nanoparticles at Karnatak University Dharwad. We are thankful to Karnatak Institute of DNA Research (KIDNAR), Dharwad for providing the instrumentation facility. We are also grateful to the Sophisticated Test and Instrumentation Center (STIC), Kochi, Kerala, for HR-TEM analysis. We are also thankful to Maratha Mandal Dental College, Belagavi, Karnataka, for providing a laboratory facility to perform an anti-TB activity to complete the present study.

Author Contributions

SDK: Draft preparation and design of work, data acquisition, statistical analysis, interpretation of data for work, writing, review and editing; TCT: Draft preparation and design of work, critical revision for important intellectual contents. All the authors read and approved the final version of manuscript.

Conflict of Interest

The authors report no conflicts of interest.

References

1. WHO tuberculosis report 2020. www.who.int/teams/global-tuberculosis-programme/tb-reports.
2. Zargarnezhad S, Gholami A, Khoshneviszadeh M, Abootalebi SN, Ghasemi Y. Antimicrobial activity of isoniazid in conjugation with surface-modified magnetic nanoparticles against mycobacterium tuberculosis and nonmycobacterial microorganisms. J Nanomater. 2020;2020(4):7372531. doi:10.1155/2020/7372531
3. Nasiruddin M, Neyaz MK, Das S. Nanotechnology-Based Approach in Tuberculosis Treatment. Tuberc Res Treat. 2017;2017:4920209. doi:10.1155/2017/4920209
4. Globocan. Lung Fact Sheet. Observatório Global do Câncer. 2020. https://gco.iarc.fr/today
5. Aziz N, Faraz M, Sherwani MA, Fatma T, Prasad R. Illuminating the anticancerous efficacy of a new fungal chassis for silver nanoparticle synthesis. Front Chem. 2019;7:65. doi:10.3389/fchem.2019.00065
6. Jain N, Jain P, Rajput D, Patil UK. Green synthesized plant-based silver nanoparticles: therapeutic prospective for anticancer and antiviral activity. Micro Nano Syst Lett. 2021;9(1):5. doi:10.1186/s40486-021-00131-6
7. Rajeshkumar S, Rinitha G. Nanostructural characterization of antimicrobial and antioxidant copper nanoparticles synthesized using novel *Persea americana* seeds. OpenNano. 2018;3:18-27. doi:10.1016/j.onano.2018.03.001
8. Banerjee P, Satapathy M, Mukhopahayay A, Das P. Leaf extract mediated green synthesis of silver nanoparticles from widely available Indian plants: Synthesis, characterization, antimicrobial property and toxicity analysis. Bioresour Bioprocess. 2014;1:3. doi:10.1186/s40643-014-0003-y
9. Suriati G, Mariatti M and Azizan A. Synthesis of silver nanoparticles by chemical reduction method:effects

of reducing agent and surfactant concentration. Int J Automot Mech Eng. 2015;10:1920-7. doi:10.1016/S0140-6736(13)61836-X.
10. Tseng KH, Lee HL, Liao CY, Chen KC, Lin HS. Rapid and efficient synthesis of silver nanofluid using electrical discharge machining. J Nanomater. 2013;2013:174939. doi:10.1155/2013/174939
11. Jia H, Zeng J, Song W, An J, Zhao B. Preparation of silver nanoparticles by photo-reduction for surface-enhanced Raman scattering. Thin Solid Films. 2006;496(2):281-7. doi:10.1016/j.tsf.2005.08.359
12. Firdhouse MJ, Lalitha P. Biosynthesis of silver nanoparticles and its applications. J Nanotechnol. 2015;2015:829526. doi:10.1155/2015/829526
13. Hemlata, Meena PR, Singh AP, Tejavath KK. Biosynthesis of silver nanoparticles using *Cucumis prophetarum* aqueous leaf extract and their antibacterial and antiproliferative activity against cancer cell lines. ACS Omega. 2020;5(10):5520-8. doi:10.1021/acsomega.0c00155
14. Moodley JS, Krishna SBN, Pillay K, Sershen, Govender P. Green synthesis of silver nanoparticles from *Moringa oleifera* leaf extracts and its antimicrobial potential. Adv Nat Sci Nanosci Nanotechnol. 2018;9(1):015011. doi:10.1088/2043-6254/aaabb2
15. Bharathi D, Diviya Josebin M, Vasantharaj S, Bhuvaneshwari V. Biosynthesis of silver nanoparticles using stem bark extracts of *Diospyros montana* and their antioxidant and antibacterial activities. J Nanostructure Chem. 2018;8(1):83-92. doi:10.1007/s40097-018-0256-7
16. Joshi N, Chhabra J. Biological synthesis of silver nanoparticles using the tuberous root extract of *Ipomoea batatas* and their characterizations and antibacterial activity. Asian J Pharm Clin Res. 2019;12(6):300-3. doi:10.22159/ajpcr.2019.v12i6.33561
17. Ali ZA, Yahya R, Sekaran SD, Puteh R. Green synthesis of silver nanoparticles using apple extract and its antibacterial properties. Adv Mater Sci Eng. 2016;2016:4102196. doi:10.1155/2016/4102196
18. Padalia H, Moteriya P, Chanda S. Green synthesis of silver nanoparticles from marigold flower and its synergistic antimicrobial potential. Arab J Chem. 2015;8(5):732-41. doi:10.1016/j.arabjc.2014.11.015
19. Burlacu E, Tanase C, Coman NA, Berta L. A review of bark-extract-mediated green synthesis of metallic nanoparticles and their applications. Molecules. 2019;24(23):4354. doi:10.3390/molecules24234354
20. Khatami M, Pourseyedi S, Khatami M, Hamidi H, Zaeifi M, Soltani L. Synthesis of silver nanoparticles using seed exudates of *Sinapis arvensis* as a novel bioresource, and evaluation of their antifungal activity. Bioresour Bioprocess. 2015;2(1):19. doi:10.1186/s40643-015-0043-y
21. Chavata R, Datchanamurthy S, Kotteeswaran V. Biofabrication of silver nanoparticles from aqueous leaf extract of *Leucas aspera* and their anticancer activity on human cervical cancer cells. Adv Nat Sci Nanosci Nanotechnol. 2019;10(4):045008. doi:10.1088/2043-6254/ab5103
22. Gloria EC, Ederley V, Gladis M, César H, Jaime O, Oscar A, et al. Synthesis of silver nanoparticles (AgNPs) with antibacterial activity. J Phys Conf Ser. 2017;850(1):012023. doi:10.1088/1742-6596/850/1/012023
23. Roy P, Das B, Mohanty A, Mohapatra S. Green synthesis of silver nanoparticles using *Azadirachta indica* leaf extract and its antimicrobial study. Appl Nanosci. 2017;7(8):843-50. doi:10.1007/s13204-017-0621-8
24. Ponarulselvam S, Panneerselvam C, Murugan K, Aarthi N, Kalimuthu K, Thangamani S. Synthesis of silver nanoparticles using leaves of *Catharanthus roseus* Linn. G. Don and their antiplasmodial activities. Asian Pac J Trop Biomed. 2012;2(7):574-80. doi:10.1016/S2221-1691(12)60100-2
25. Devi M, Devi S, Sharma V, Rana N, Bhatia RK, Bhatt AK. Green synthesis of silver nanoparticles using methanolic fruit extract of Aegle marmelos and their antimicrobial potential against human bacterial pathogens. J Tradit Complement Med. 2020;10(2):158-65. doi:10.1016/j.jtcme.2019.04.007
26. Elhawary S, El-Hefnawy H, Mokhtar FA, Sobeh M, Mostafa E, Osman S, et al. Green synthesis of silver nanoparticles using extract of *Jasminum officinal* l. Leaves and evaluation of cytotoxic activity towards bladder (5637) and breast cancer (mcf-7) cell lines. Int J Nanomedicine. 2020;15:9771-81. doi:10.2147/IJN.S269880
27. Masum MI, Siddiqa MM, Ali KA, Zhang Y, Abdallah Y, Ibrahim E, et al. Biogenic synthesis of silver nanoparticles using *Phyllanthus emblica* fruit extract and its inhibitory action against the pathogen acidovorax oryzaestrain RS-2 of rice bacterial brown stripe. Front Microbiol. 2019;10:820. doi:10.3389/fmicb.2019.00820
28. Menon S, Agarwal H, Rajesh Kumar S, Venkat Kumar S. Green synthesis of silver nanoparticles using medicinal plant *Acalypha indica* leaf extracts and its application as an antioxidant and antimicrobial agent against foodborne pathogens. Int J Appl Pharm. 2017;9(5):42-50. doi:10.22159/ijap.2017v9i5.19464
29. Kumar VR, Venkatachalam V V. Physicochemical evaluation and phytochemical investigation of the leaves of *Grewia tiliaefolia* Vahl. Der Pharmacia Lettre. 2016;8(20):52-6.
30. 30. Ullah W, Uddin G, Siddiqui BS. Pharmacological and phytochemical profile of genus Grewia. J Asian Nat Prod Res. 2012;14:37-41. doi:10.1080/10286020.2011.639764
31. Thamizh SN, Vengatakrishnan V, Murugesan S, Damodar KS. Antioxidant and antiproliferative activity of methanolic extract of *Grewia tiliaefolia* (Vahl) bark in different cancer cell lines. Int J Pharm Life Sci.

2010;1(2):54-60.
32. Dicson SM, Samuthirapandi M, Govindaraju A, Kasi PD. Evaluation of in vitro and in vivo safety profile of the Indian traditional medicinal plant *Grewia tiliaefolia*. Regul Toxicol Pharmacol. 2015;73(1):241-7. doi:10.1016/j.yrtph.2015.07.011
33. Khadeer MB, Krishna V, Dandin CJ. In vitro antioxidant and in vivo prophylactic effects of two γ -lactones isolated from *Grewia tiliaefolia* against hepatotoxicity in carbon tetrachloride intoxicated rats. Eur J Pharmacol. 2010;631(1-3):42-52. doi:10.1016/j.ejphar.2009.12.034
34. Vivek Y, Vinay P, Vijayan P. Antioxidant , antimicrobial and cytotoxicity properties of the methanolic extract from *Grewia tiliaefolia* Vahl. Pharmacogn Mag. 2008;4(16):329-34.
35. Sarkar S, Kotteeswaran V. Green synthesis of silver nanoparticles from aqueous leaf extract of Pomegranate (*Punica granatum*) and their anticancer activity on human cervical cancer cells. Adv Nat Sci Nanosci Nanotechnol. 2018;9(2):025014. doi:10.1088/2043-6254/aac590
36. Choi CW, Kim SC, Hwang SS, Choi BK, Ahn HJ, Lee MY, et al. Antioxidant activity and free radical scavenging capacity between Korean medicinal plants and flavonoids by assay-guided comparison. Plant Sci. 2002;163(6):1161-8. doi:10.1016/S0168-9452(02)00332-1
37. Shettar AK, Madagi SB, Vedamurthy AB. Phytochemical screening and in-vitro antioxidant and antiproliferative activity of aqueous leaf extract of *Ximtenia americana* against non-small cell lung cancer. Cancer Surg. 2018;03:1. doi:10.4172/2573-542x.1000117
38. Lourenço MCS, De Souza MVN, Pinheiro AC, Ferreira MDL, Gonçalves RSB, Nogueira TCM, et al. Evaluation of anti-tubercular activity of nicotinic and isoniazid analogues. Arkivoc. 2007;2007(15):181-91. doi:10.3998/ark.5550190.0008.f18
39. Al-Shmgani HSA, Mohammed WH, Sulaiman GM, Saadoon H, Mohammed WH, Sulaiman GM. Biosynthesis of silver nanoparticles from *Catharanthus roseus* leaf extract and assessing their antioxidant, antimicrobial, and wound-healing activities. Artif Cells Nanomed Biotechnol. 2016;45(6):1-7. doi:10.1080/21691401.2016.1220950
40. Majeed S, Fadlin N, Bakhtiar B, Danish M, Ibrahim MNM, Hashim R. Green approach for the biosynthesis of silver nanoparticles and its antibacterial and antitumor effect against osteoblast MG-63 and breast MCF- 7 cancer cell lines. Sustain Chem Pharm. 2019;12:100138. doi:10.1016/j.scp.2019.100138
41. Sumi Maria B, Devadiga A, Shetty Kodialbail V, Saidutta MB. Synthesis of silver nanoparticles using medicinal *Zizyphus xylopyrus* bark extract. Appl Nanosci. 2015;5(6):755-62. doi:10.1007/s13204-014-0372-8
42. Qasim NM, Zohra T, Khalil AT, Saqib S, Ayaz M, Ahmad A, et al. *Seripheidium quettense* mediated green synthesis of biogenic silver nanoparticles and their theranostic applications. Green Chem Lett Rev. 2019;12(3):310-22. doi:10.1080/17518253.2019.1643929
43. Khorrami S, Zarrabi A, Khaleghi M, Danaei M, Mozafari MR. Selective cytotoxicity of green synthesized silver nanoparticles against the MCF-7 tumor cell line and their enhanced antioxidant and antimicrobial properties. Int J Nanomedicine. 2018;13:8013-24. doi:10.2147/IJN.S189295
44. Haque MN, Kwon S, Cho D. Formation and stability study of silver nano-particles in aqueous and organic medium. Korean J Chem Eng. 2017;34(7):2072-8. doi:10.1007/s11814-017-0096-z
45. Abo-Elmagd RA, Hussein MH, Hamouda RA, Shalan AE, Abdelrazak A. Statistical optimization of photo-induced biofabrication of silver nanoparticles using the cell extract of: *Oscillatoria limnetica*: insight on characterization and antioxidant potentiality. RSC Adv. 2020;10(72):44232-46. doi:10.1039/d0ra08206f
46. Pirtarighat S, Ghannadnia M, Baghshahi S. Green synthesis of silver nanoparticles using the plant extract of *Salvia spinosa* grown in vitro and their antibacterial activity assessment. J Nanostructure Chem. 2019;9(1):1-9. doi:10.1007/s40097-018-0291-4
47. Devi DR, Battu GR. Qualitative Phytochemical screening and FTIR spectroscopic analysis of *Grewia Tilifolia* (Vahl) leaf extracts. Int J Curr Pharm Res. 2019;11(4):100-7. doi:10.22159/ijcpr.2019v11i4.34936
48. Vanaja M, Gnanajobitha G, Paulkumar K, Rajeshkumar S, Malarkodi C, Annadurai G. Phytosynthesis of silver nanoparticles by *Cissus quadrangularis*: influence of physicochemical factors. J Nanostructure Chem. 2013;3:17. doi:10.1186/2193-8865-3-17
49. Balan K, Qing W, Wang Y, Liu X, Palvannan T, Wang Y, et al. Antidiabetic activity of silver nanoparticles from green synthesis using *Lonicera japonica* leaf extract. RSC Adv. 2016;6(46):40162-8. doi:10.1039/c5ra24391b
50. Pattanayak S, Mollick MMR, Maity D, Chakraborty S, Dash SK, Chattopadhyay S, et al. *Butea monosperma* bark extract mediated green synthesis of silver nanoparticles: Characterization and biomedical applications. J Saudi Chem Soc. 2017;21(6):673-84. doi:10.1016/j.jscs.2015.11.004
51. Mata R, Reddy NJ, Rani SS. Catalytic and biological activities of green silver nanoparticles synthesized from *Plumeria alba* (frangipani) flower extract. Mater Sci Eng C. 2015;51:216-25. doi:10.1016/j.msec.2015.02.053
52. Chahardoli A, Karimi N, Fattahi A. *Nigella arvensis* leaf extract mediated green synthesis of silver nanoparticles: Their characteristic properties and biological efficacy. Adv Powder Technol. 2018;29(1):202-10. doi:10.1016/j.apt.2017.11.003
53. Venugopal K, Rather HA, Rajagopal K, Shanthi MP, Sheriff K, Illiyas M, et al. Synthesis of silver nanoparticles (Ag NPs) for anticancer activities (MCF 7 breast and A549 lung cell lines) of the crude extract of

Syzygium aromaticum. J Photochem Photobiol B Biol. 2017;167:282-9. doi:10.1016/j.jphotobiol.2016.12.013
54. Krishnan V, Bupesh G, Manikandan, Thanigai AK, Magesh S KR and MM. Green Synthesis of Silver Nanoparticles Using *Piper nigrum* Concoction and its Anticancer Activity against MCF-7 and Hep-2 Cell Lines. J Antimicrob Agents. 2016;2(3):8-12. doi:10.4172/2472-1212.1000123
55. Sukirtha SR, Priyanka KM, Antony JJ, Kamalakkannan S, Thangam R, Gunasekaran P, et al. Cytotoxic effect of Green synthesized silver nanoparticles using *Melia azedarach* against in vitro HeLa cell lines and lymphoma mice model. Process Biochem. 2012;47(2):273-9. doi:10.1016/j.procbio.2011.11.003
56. Alavi M, Rai M, Martinez F, Kahrizi D, Khan H, Rose I. The efficiency of metal , metal oxide, and metalloid nanoparticles against cancer cells and bacterial pathogens : different mechanisms of action. Cell Mol Biomed Rep. 2022;2(1):10-21. doi:10.55705/CMBR.2022.147090.1023
57. Abdel-Aziz MM, Elella MHA, Mohamed RR. Green synthesis of quaternized chitosan/silver nanocomposites for targeting *Mycobacterium tuberculosis* and lung carcinoma cells (A-549). Int J Biol Macromol. 2020;142:244-53. doi:10.1016/j.ijbiomac.2019.09.096
58. Jung WK, Koo HC, Kim KW, Kim SH, Park YH, Jung WK, et al. Antibacterial activity and mechanism of action of the silver ion in *Staphylococcus aureus* and *Escherichia coli*. 2008;74(7):2171-8. doi:10.1128/AEM.02001-07
59. Singh R, Nawale LU, Arkile M, Shedbalkar UU, Wadhwani SA, Sarkar D, et al. Chemical and biological metal nanoparticles as antimycobacterial agents: A comparative study. Int J Antimicrob Agents. 2015;46(2):183-8. doi:10.1016/j.ijantimicag.2015.03.014
60. Patil BN, Taranath TC. *Limonia acidissima* L. leaf mediated synthesis of zinc oxide nanoparticles : A potent tool against *Mycobacterium tuberculosis*. Int J Mycobacterio. 2016;5(2):197-204. doi:10.1016/j.ijmyco.2016.03.004
61. Alavi M. Rai M. Antisense RNA, the modified CRISPR-Cas9, and metal/metal oxide nanoparticles to inactivate pathogenic bacteria. Cell Mol Biomed Rep. 2021;1(2):52-9. doi:10.55705/CMBR.2021.142436.1014
62. Rosman NSR, Harun NA, Idris I, Ismail WIW. Eco-friendly silver nanoparticles (AgNPs) fabricated by green synthesis using the crude extract of marine polychaete, *Marphysa moribidii*: biosynthesis, characterisation, and antibacterial applications. Heliyon. 2020;6(11):e05462. doi:10.1016/j.heliyon.2020.e05462